

DOI: 10.1515/amm-2016-0164

M. MIKUŚKIEWICZ*, M. STOPYRA*#, G. MOSKAL*

SYNTHESIS AND THERMAL PROPERTIES OF CERIUM-DYSPROSIUM OXIDE

The paper presents results of investigation on synthesis and characterization of cerium-dysprosium oxide. The input powders – dysprosium oxide Dy_2O_3 and cerium oxide CeO_2 – were mixed so as to obtain equimolar ratio of cations, milled in alcohol and synthesized via solid state reaction process at $1350^\circ C$ under 15MPa in vacuum for 2h. The microstructure, phase composition and thermal properties were analyzed. The obtained material was multiphase. Non-stoichiometric compounds were identified. Thermal diffusivity of investigated material decreased in the temperature range of $25-1000^\circ C$ from 0,71 to 0,45 mm^2/s .

Keywords: cerium oxide, dysprosium oxide, thermal properties, TBC

1. Introduction

The efficiency of aircraft engines strongly depends on the temperature in combusting chamber, therefore in order to limit the fuel consumption and exhaust gases emission the operating parameters of engine need to be increased. However, the higher the temperature, the more advanced heat resistant materials are required. As the operating temperature excess the upper limit of Ni-based superalloys, the ceramic coatings are applied on the crucial engine parts. In the modern aircraft engine turbines thermal barrier coatings (TBC) are commonly used. TBCs in general are double-layer systems, where the outer layer (top-coat) is designed to thermally insulate the base material [1-3]. The requirements for top-coat material are low heat conductivity, resistance to chemically aggressive environment at high temperature, resistance to thermo-mechanical fatigue and long-term stability of phase composition [1-3]. These coatings are usually plasma-sprayed [4] and the typical material for the top-coat is yttria-stabilized zirconia (8YSZ) [5]. The increasing requirements for the engine operating parameters implies the necessity of developing new materials, with increasingly better insulating properties.

One of the material solution proposed for the new TBC systems are binary oxides with fluorite (F) or pyrochlore (P) type crystal structure and general formula $A_2B_2O_7$ [6], where the A-site is occupied by larger 3^+ cations and the B-site by the smaller 4^+ cations. The difference between pyrochlore and fluorite crystal structure lies in the ordering both in cationic and anionic array, where the oxygen vacancies occur at 8a site [7]. Thereby, pyrochlore crystal structure can be distinguished from fluorite by the presence of superstructure. The stability of P-type structure is governed by the ratio of cation radii r_A/r_B . It

is generally assumed that the systems with $r_A/r_B < 1.48$ exhibit F-type structure, while the values in the range from 1.48 to 1.76 result in P-type structure, wherein ordering of crystal structure depends also on material's thermal history and stoichiometry [7]. The representatives of this group of materials, proposed as top-coat candidates are rare earth metals zirconates [6].

There are plenty of methods for synthesis of rare earth metal pyrochlores and fluorites. They can be generally divided into 2 groups: solid-state-reaction (SSR) and wet-chemistry methods. The input materials in SSR methods are oxide powders, which are mixed in appropriate proportions, homogenized and finally sintered. These methods are relatively simple, but the structure of final product is often inhomogeneous. In the chemical methods (e.g. co-precipitation, sol-gel) the powders are obtained from liquid solutions. Precursors are dissolved and mixed at molecular level which enhances homogeneity [8]. However, the reagents are often more expensive, therefore these methods are preferred when high homogeneity and not necessary large amount of material is needed.

Thermal properties of some of the RE binary oxides with P or F type of structure have been already well characterized in available literature. Among them they are gadolinium [9], neodymium [10], samarium [11] and dysprosium [12] zirconates, mostly obtained via conventional solid state reaction route. However, there are much less information about compounds from dysprosia-ceria ($Dy_2O_3-CeO_2$) system. Ceria is the only one among rare earth oxides which exhibit 4^+ instead of 3^+ oxidation state. Therefore it can occupy B site in $A_2B_2O_7$ compounds. It is also known, that due to large ionic radius of Ce, no P phase is present in any Ce-RE system. In work [13] it was proved, that increasing amount of Dy in $(Sm_{(1-x)}Dy_x)_2Ce_2O_7$ prepared by

* SILESIAAN UNIVERSITY OF TECHNOLOGY, FACULTY OF MATERIALS ENGINEERING AND METALLURGY, 8 KRASINSKIEGO STR., 40-019 KATOWICE, POLAND

Corresponding author: michal.stopyra@polsl.pl

SSR method causes decrease in thermal diffusivity. The aim of this work was synthesis, structural and thermal characterization of Dy-Ce binary oxide.

2. Material for the research and experimental procedure

Nano-crystalline input powders – dysprosium oxide (99,9%, Hefei EV NANO Technology) and cerium oxide (99,9% Hefei EV NANO Technology) were mixed so that Ce:Dy molar ratio was 1:1 and wet-milled in mortar with alcohol. Final product was obtained via solid state reaction in high temperature vacuum press “Degussa” VSPi-15/20 (1350°C/15MPa/2h). Calorimetric studies (DSC 404 F1 Netzsch) were performed for feedstock powders and their mixture after milling. The phase identification of sintered material was carried out using X-ray diffraction (XRD, Jeol JDX-7S diffractometer). The microstructure was investigated using scanning electron microscope (SEM, Hitachi

S-3400N) equipped with energy dispersion spectrometer (EDS, Thermo Noran System Six). Thermal diffusivity was measured using Laser-Flash method (LFA 427) in the temperature range 25 – 1400°C.

3. Results and discussion

The results of DSC analysis of powders are presented in Fig. 1. No significant difference in calorimetric curves for the feedstock powders. Small exothermic peak with maximum at 900°C occurs in both oxides. In the mixture this peak is also present but barely visible. This is probably caused by mutual dissolution of constituent oxides.

Fig. 2 presents microstructure of synthesized material after sintering at 1350°C under 15 MPa. As indicated by the diversity in brightness in BSE images, the obtained material is inhomogeneous and multi-phase. EDS analysis was conducted

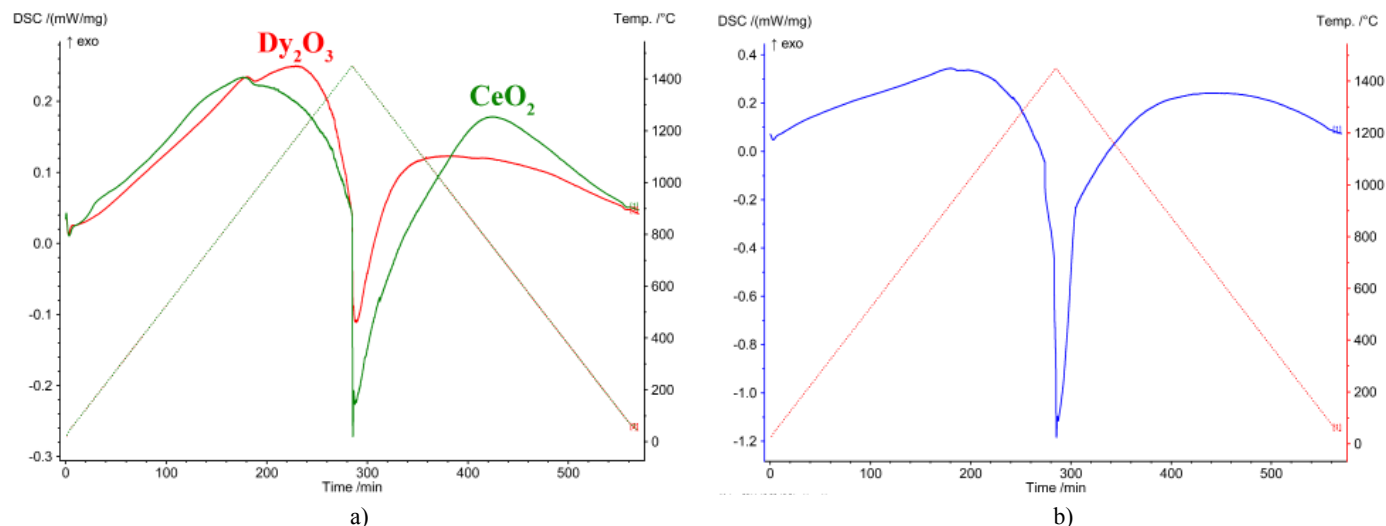


Fig. 1. DSC curves: Dy₂O₃ and CeO₂ (a) and their mixture after milling (b)

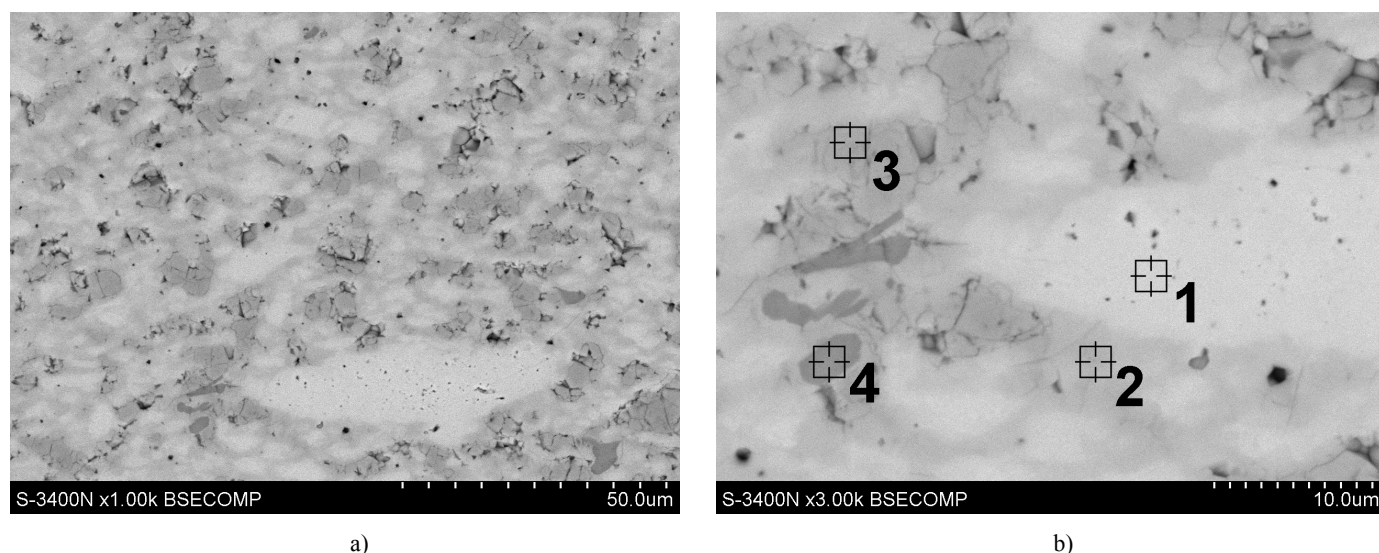


Fig. 2. Microstructure of Dy₂O₃-CeO₂ sintered pellets with marked spots for EDS analysis

in 4 representative spots marked in Fig. 2b and the results are presented in Fig. 3. The brightest areas (no. 1) were Dy-rich and the darkest (no. 4) were Ce-rich with c.a. 39% at. Cl content (probably impurity from CeO₂ feedstock powder). In areas marked by no 2 the Ce/Dy ratio was closest to 1. Additionally EDS line-scan was performed along Ce-rich area (Fig. 4), probably unreacted ceria. It can be seen that dysprosium is present

along the whole line, which suggests this is the solid solution of dysprosia in ceria.

Based on SEM and EDS results it can be stated that the mixture of powders was not homogenized well enough. They are micrometric-sized areas enriched with one of constituent oxides separated from another by the areas with intermediate chemical composition.

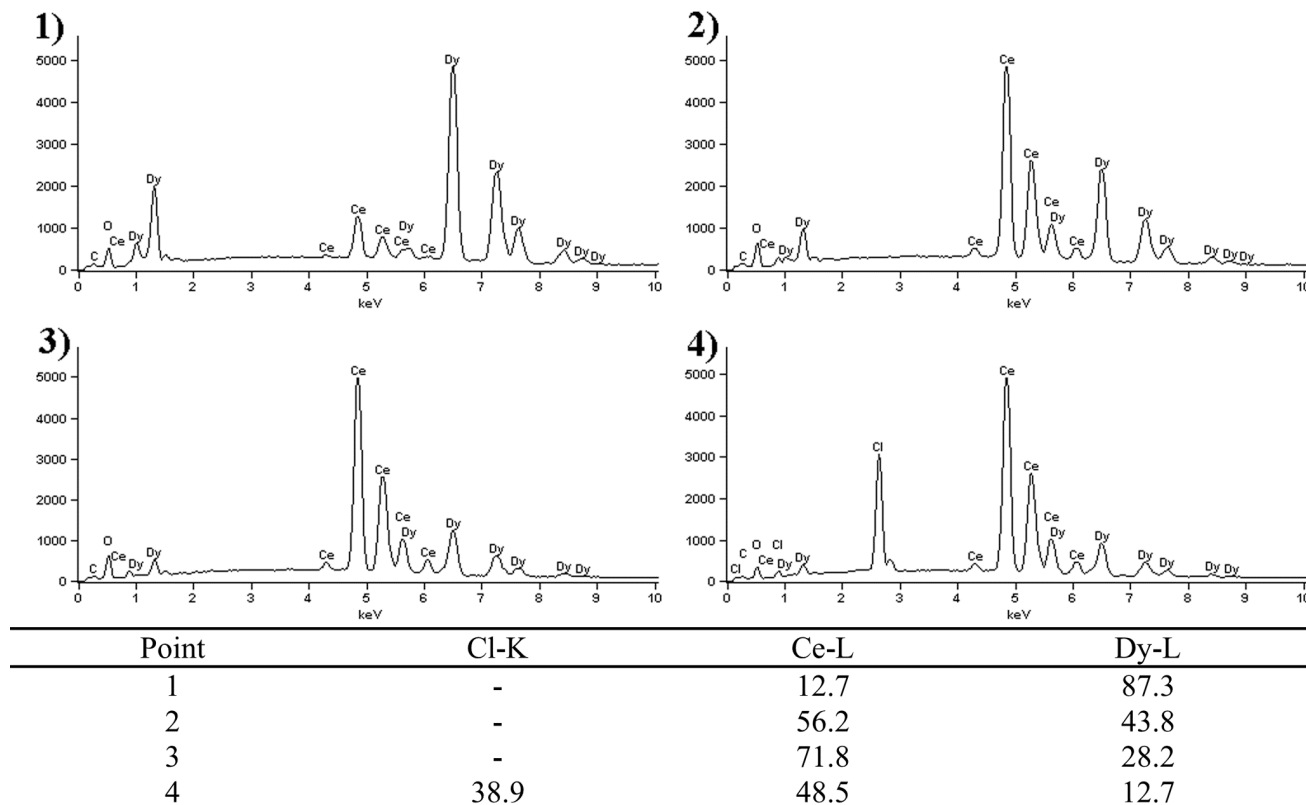


Fig. 3. Qualitative and quantitative results of EDS analysis in points marked in Fig. 2b

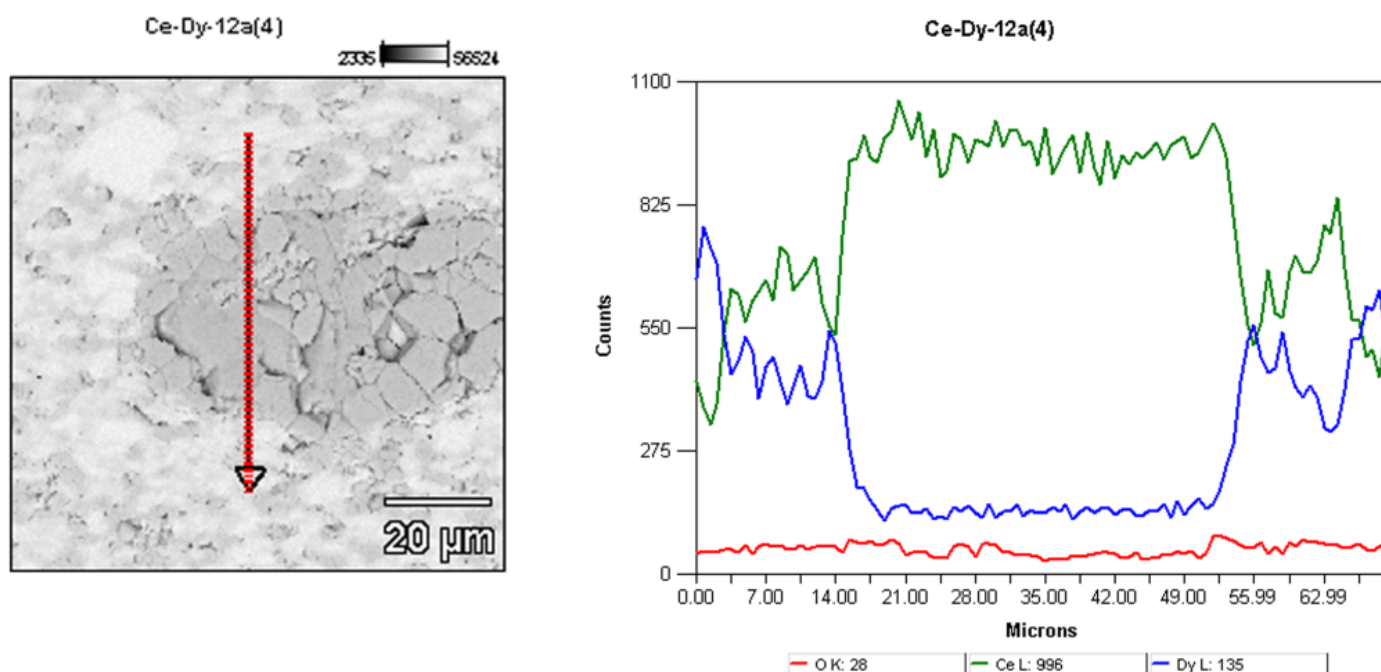


Fig. 4. EDS linescan in Ce-rich area

The X-ray diffraction analysis (Fig. 5) revealed the presence of 3 phases. The most intensive peaks were assigned to binary, non-stoichiometric oxide $\text{Ce}_{0.8}\text{Dy}_{0.2}\text{O}_{1.9}$ and $\text{Ce}_{0.5}\text{Dy}_{0.5}\text{O}_{1.75}$, both with fluorite-type cubic structure (Fm-3m space group). These oxides has similar lattice parameter (5.411Å and 5.473Å respectively), hence they are difficult to distinguish, especially at low values of 2θ . With the increase of 2θ , the widening on the left side of the peaks becomes more visible (Fig. 6). It is

also noticeable that the location of peaks on the spectra does not exactly matches the values of 2θ angle for these compounds. This is probably caused by non-stoichiometry of the obtained phases, as indicated by the results of EDS analysis. Another identified phase was dysprosium oxide Dy_2O_3 (Ia3 space group). The intensity of its peaks is weak which indicates that majority of Dy_2O_3 dissolved in CeO_2 and formed new phases.

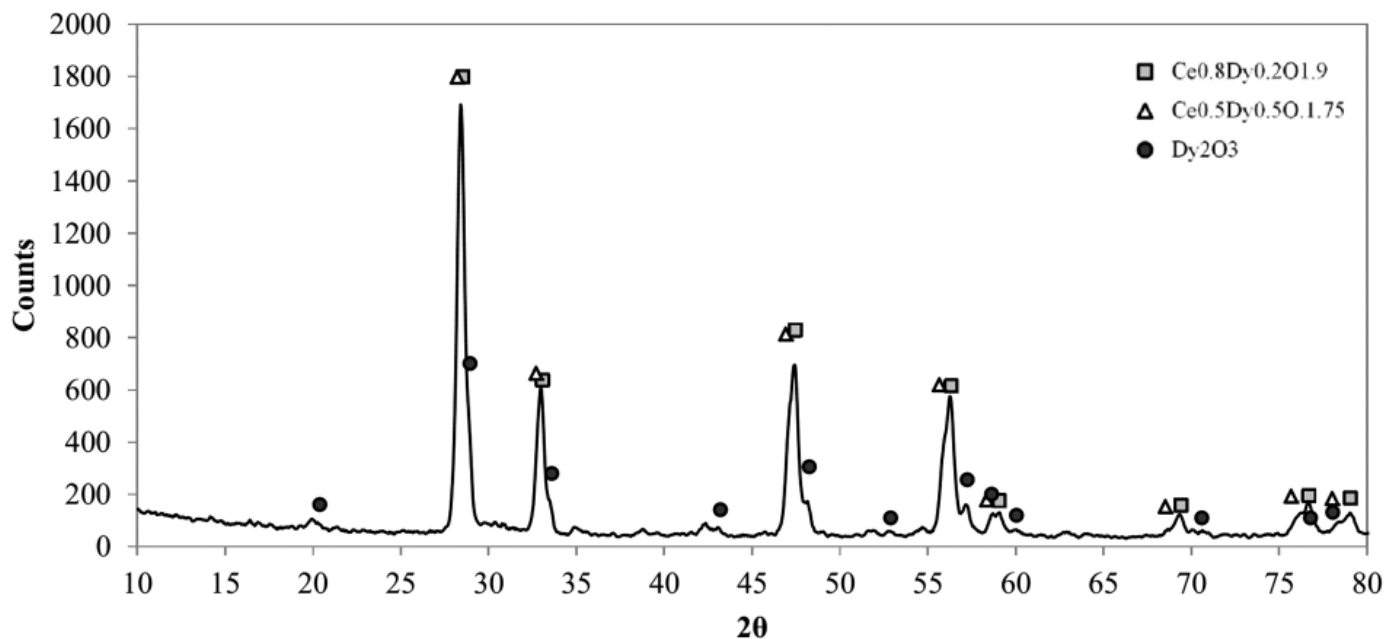


Fig. 5. XRD results of Dy_2O_3 - CeO_2 sintered pellets

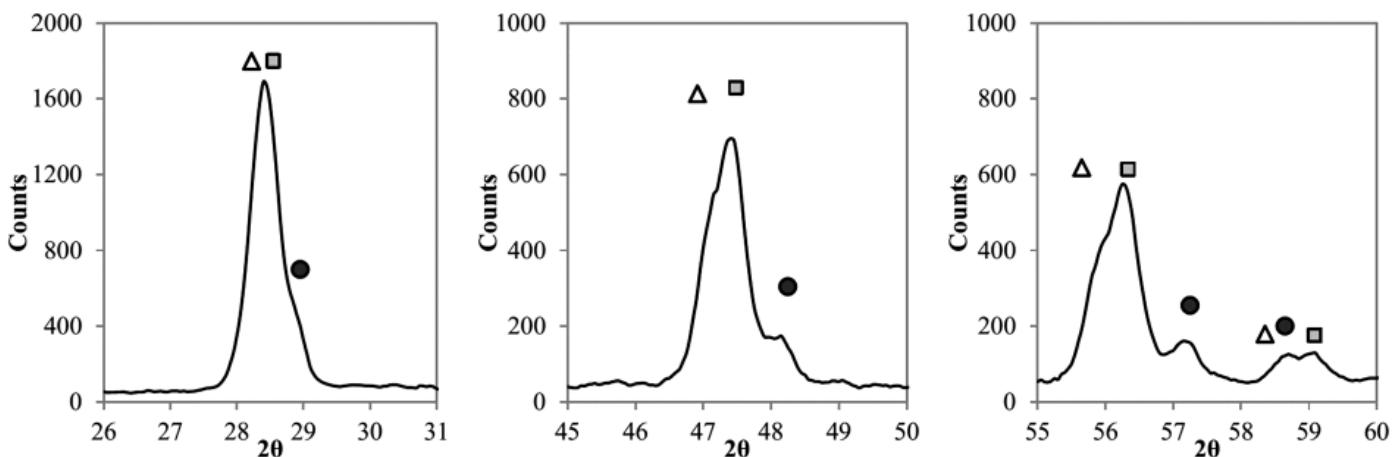


Fig. 6. Close-up of selected peaks of spectra from Fig. 5

The thermal diffusivity of obtained material was measured in temperature range 25 – 1400°C, the results are presented in Fig. 7. At room temperature the κ value was 0.71 mm^2/s and it gradually decreased to 0.45 mm^2/s at 1000°C. The shape of thermal diffusivity curve suggests that κ value decrease in accordance to the function of $\kappa = f(T^{-1})$. It suggests that thermal

resistance of investigated material is related to phonon scattering as a dominating mechanism [14-16]. The further increase up to 0.61 mm^2/s at 1400°C is caused by the increasing share of radiation heat transfer at high temperature. The obtained materials has lower thermal diffusivity than Dy-modified $\text{Sm}_2\text{Ce}_2\text{O}_7$ in whole temperature range [13].

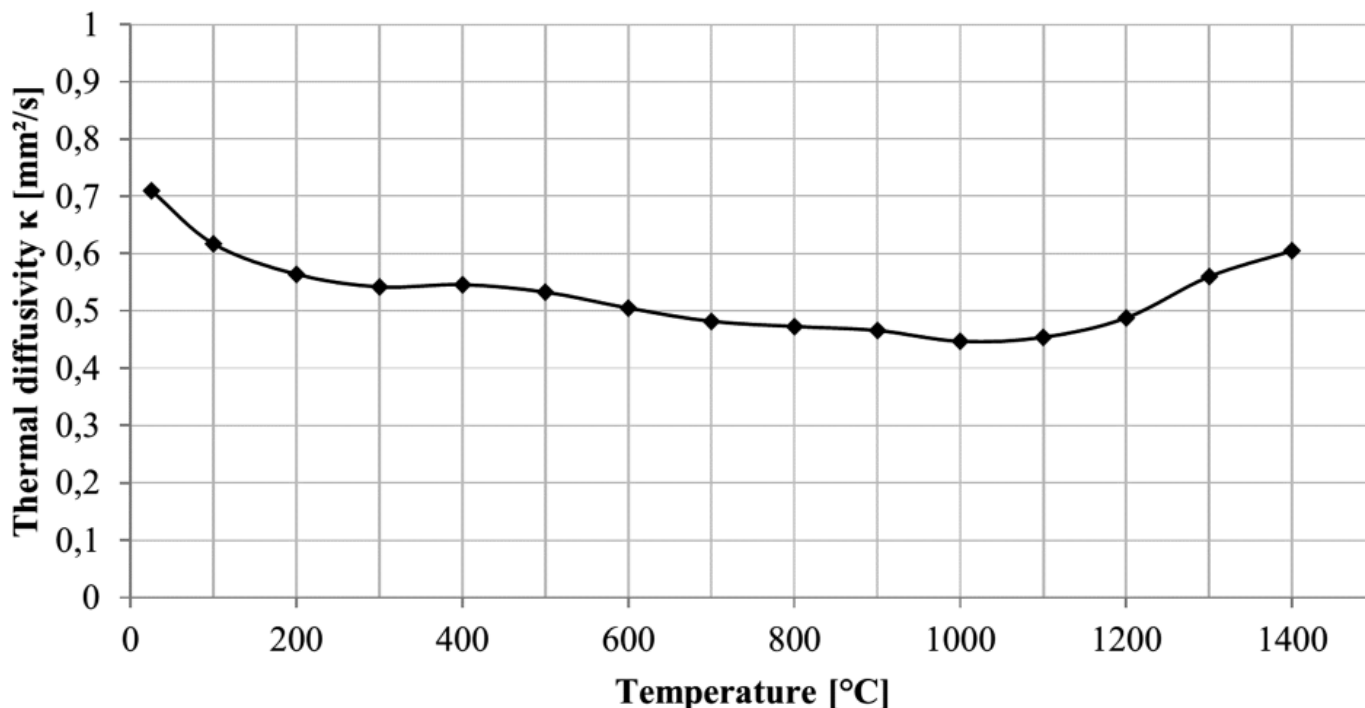


Fig. 7. Thermal diffusivity of synthesized Ce-Dy oxide at different temperatures

4. Conclusions

The binary Ce-Dy oxide was synthesized via solid state reaction. The milling in ethanol of constituent oxides did not provide appropriate homogenization of the mixture. As a result, the obtained material exhibited chemical inhomogeneity. Due to the mutual dissolution of cerium and dysprosium oxides, microstructure of sintered material consisted of Ce and Dy-rich areas separated by the areas with intermediate chemical composition and the ratio of Ce/Dy %_{at.} close to 1. The presence of Ce_{0.8}Dy_{0.2}O_{1.9}, Ce_{0.5}Dy_{0.5}O_{1.75} and Dy₂O₃ was revealed as well. However, considering the chemical composition in micro-areas, other non-stoichiometric phases with fluorite-type structure and similar lattice parameter could be present. Thermal diffusivity decreased from 0,71 mm² at 25°C to 0,45 mm²/s at 1000°C. Future works will focus on obtaining single-phase binary oxide and further increase in insulating properties.

Acknowledgment

This work was supported by Institute of Materials Science of Silesian University of Technology, as a part of Statutory Research no BK232/RM3/2014.

REFERENCES

- [1] C.U. Hardwicke, Y.C. Lau, *J. Therm. Spray Techn.* **22**, 564 (2013).
- [2] D.R. Clarke, S.R. Phillpot, *Mater. Today* **8**(6), 22 (2005).
- [3] Ch.W. Siry, H. Wanzek, C.-P. Dau, *Materialwiss. Werkst.* **32**, 650 (2001).
- [4] G. Moskal, A. Grabowski, *Key Eng. Mat.* **465**, 219 (2011).
- [5] X.Q. Cao, R. Vassen, D. Stoeber, *J. Eur. Ceram. Soc.* **24**, 1 (2004).
- [6] J.W. Fergus, *Metall. Mater. Trans. E* **1**, 118 (2014).
- [7] C.R. Stanek. *Atomic Scale Disorder in Fluorite and Fluorite Related Oxides*. PhD Thesis, Imperial College of Science, Technology and Medicine. London SW7 2AZ, August 2003.
- [8] L. Kong, I. Karatchevtseva, D.J. Gregg, M.G. Blackford, R. Holmes, G. Triani, *J. Eur. Ceram. Soc.* **33**, 3273 (2013).
- [9] G. Moskal, L. Swadźba, M. Hetmańczyk, B. Witala, B. Mendala, J. Mendala, P. Sosnowy, *J. Eur. Ceram. Soc.* **32**, 2035 (2012).
- [10] G. Moskal, L. Swadźba, M. Hetmańczyk, B. Witala, B. Mendala, J. Mendala, P. Sosnowy, *J. Eur. Ceram. Soc.* **32**, 2025 (2012).
- [11] G. Moskal, M. Mikuśkiewicz, *Defect Diffus. Forum* **336**, 91 (2013).
- [12] M. Mikuśkiewicz, M. Stopyra, G. Moskal, *Solid State Phenom.* **223**, 54 (2015).
- [13] Z. Hongsong, Y. Shuqing, C. Xiaoge, *J. Eur. Ceram. Soc.* **34**, 55 (2014).
- [14] P.G. Klemens, *A Theory of the thermal conductivity of solids*, in R.P. Tye (Ed.), *Thermal Conductivity vol. 1*, Academic Press (1969).
- [15] C. Kittel, *Introduction to solid state physics*, Wiley, 1986.
- [16] G.A. Slack, *Solid State Phys.* **34**, 1 (1979).